

Structural Design for Disaster Resilience

Fahim Sadek, Joseph A. Main, John L. Gross, and Therese P. McAllister

Engineering Laboratory, National Institute of Standards and Technology, Gaithersburg, Maryland,
20899-8611, USA

ABSTRACT

This paper presents a brief overview of research at the National Institute of Standards and Technology (NIST) on disaster resilience of buildings, infrastructure, and communities, including component programs and projects. NIST's efforts aim at developing the scientific basis required to enable technological innovation, improve predictive capabilities, and improve codes, standards, and practices for the cost-effective improvement of disaster resilience, including life-safety and reduction of property loss due to natural and man-made hazards. The fundamental idea underpinning this research is that disaster resilience can be enhanced by developing a robust capability to predict the effects of hazards on the performance of complex structural systems. This will be achieved by providing data to characterize the hazard, validated models to predict performance, metrics for measuring performance, acceptance criteria for differing levels of performance objectives, and mitigation strategies based on performance evaluation. Special emphasis is provided for two key research efforts related to structural design for disaster resilience currently underway at the NIST. These include mitigation of disproportionate collapse and fire performance of structures. For each effort, an overview is provided, followed by details of recent work carried out by the NIST including experiments and computational studies for the assessment of disproportionate collapse potential and the design and construction of the National Fire Research Laboratory (NFRL).

KEYWORDS

Computational modeling, disaster resilience, disproportionate collapse, experiments, performance based design, structural fire, structural performance.

INTRODUCTION

Despite significant progress in science and technology related to disaster-mitigation, natural and technological disasters in the United States are responsible for an estimated \$57 B (and growing) in average annual costs in terms of lives lost, disruption of commerce and financial networks, properties destroyed, and the cost of mobilizing emergency response personnel and equipment. Natural hazards are a continuing and significant threat to U.S. communities. Major catastrophes such as Hurricane Katrina (2005) and future earthquakes like the ones that struck Tohoku and Kobe, Japan in 2011 and 1995, respectively, can cause mega-losses (\$80B-\$300B) in a single event. Human activities that are accidental, criminal, or terrorist can also lead to disastrous losses. The risk across large, disaster-prone regions of the U.S. is substantially greater now than ever before due to the combined effects of urban development and population growth. In addition, much of the nation's physical infrastructure is located in parts of the country that are susceptible to natural hazards (e.g., along coastlines, in the wildland-urban interface, and in earthquake-prone regions) and significant parts of this infrastructure are aging, diminishing their capacity to resist hazards.

Disaster resilience, the ability to withstand the impacts of natural or man-made hazards and recover quickly to pre-disaster societal functions, is at once a local and a national issue. Just as the effects of a natural disaster cascade locally through impacted infrastructure and society, they can also cascade across entire regions and even nationally. Regional and national disaster resilience are impacted by pre-event mitigation, immediate response, and long-term recovery. As projected losses continue to rise, there is increasing recognition of the need to minimize the time and cost required for response and recovery by proactively identifying hazards that pose threats and acting to mitigate their potential impact. Preventing hazards (e.g., earthquakes, hurricanes, and community-scale fires) from becoming disasters depends upon the disaster resilience of our buildings and infrastructure. This, in turn, depends upon the capacity to prepare for and mitigate the impacts of hazards, preventing them from becoming disasters.

The Engineering Laboratory of the National Institute of Standards and Technology (NIST) has “Disaster Resilient Buildings, Infrastructure, and Communities” as one of its primary strategic goals. This paper presents a brief overview of this research goal including its component programs and projects. Special emphasis is provided for two key elements of this research goal related to structural design for disaster resilience: mitigation of disproportionate collapse and fire resistance of building structures.

NIST'S WORK ON DISASTER RESILIENCE

NIST's “Disaster Resilient Buildings, Infrastructure, and Communities” strategic goal aims at developing the scientific basis required to enable technological innovation, improve predictive capabilities, and improve codes, standards, and practices for the cost-effective improvement of disaster resilience, including life-safety and reduction of property loss due to natural and man-made hazards. The fundamental idea underpinning this research is that disaster resilience can be enhanced by developing a robust capability to predict the effects of hazards on the performance of complex structural systems. This will be achieved by providing data to characterize the hazard, validated models to predict performance, metrics for measuring performance, acceptance criteria for differing levels of performance objectives, and mitigation strategies based on performance evaluation. The key elements of this research goal include the following programs:

- Fire risk reduction in communities: with a focus on reducing community fire risk by increasing the fire resilience of wildland-urban interface (WUI) communities and enhancing the safety and effectiveness of firefighters. Examples of research efforts in this program include enhanced effectiveness of firefighting tactics, smart firefighting, reduced ignition of

wildland-urban fires, WUI fire data collection and exposure modeling, and WUI building and fire codes and standards.

- Fire risk reduction in buildings: with a focus on increasing the safety of building occupants and the performance of structures and their contents by enabling performance based design methodologies and innovative, cost-effective fire protection technologies. Examples of research efforts in this program include advanced fire detection, fire modeling for performance-based design, safety of building occupants, performance-based design of structures in fire, and the National Fire Research Laboratory (NFRL) which allows testing of real-scale structures under realistic mechanical and fire loading conditions (more details are provided later in the paper).
- Earthquake risk reduction in buildings and infrastructure: with a focus on developing and deploying performance-based tools, guidelines, and standards for designing buildings to resist earthquake effects, improve building safety, and enhance disaster resilience. The program fulfills the NIST applied research role in the statutory four-agency National Earthquake Hazards Reduction Program (NEHRP), including NIST's role as the NEHRP Lead Agency, and involves in-house and extramural research concentrated in five major areas: technical support for building code development, performance-based seismic engineering, national design guideline development, evaluated technology knowledge dissemination, and evaluation and strengthening for existing buildings.
- Structural performance under multi-hazards: with a focus on enhancing disaster resilience through development of prediction and evaluation tools for structural performance under a wide variety of hazards, and deriving lessons learned from disasters and failures involving structures. Examples of research efforts in this program include mitigation of disproportionate structural collapse, extreme wind engineering, coastal inundation, multi-hazard failure analysis, and disaster and failure studies.

The next sections provide details on two key research efforts related to structural design for disaster resilience currently underway at the NIST as part of the disaster resilience goal. These include mitigation of disproportionate collapse and fire performance of structures. For each effort, an overview is provided, followed by details of recent work carried out by the NIST including experiments and computational studies for the assessment of disproportionate collapse potential and the design and construction of the National Fire Research Laboratory (NFRL).

MITIGATION OF DISPROPORTIONATE COLLAPSE

Since the destruction of the Alfred P. Murrah Federal Building in 1995, caused by a truck bomb attack (FEMA 1996), and the collapse of the World Trade Center towers in 2001, caused by the impact of large passenger jetliners (NIST 2005), the engineering community, including codes and standards development organizations and public regulatory agencies, has paid greater attention to the performance of buildings subjected to damage from abnormal events. In the U.S., the American Society of Civil Engineers Standard 7 (ASCE 2010, Section C1.4), and the guidelines of the U.S. General Services Administration (GSA 2003) and the Department of Defense (DOD 2009) provide guidance to prevent disproportionate collapse (also known as progressive collapse). Disproportionate collapse occurs when an initial local failure spreads progressively, resulting in total collapse or collapse of a disproportionately large part of a structure. Resistance to disproportionate collapse is achieved either implicitly, by providing minimum levels of strength, continuity, and ductility; or explicitly, by (1) providing alternate load paths so that local damage is absorbed and major collapse is averted or (2) providing sufficient strength to structural members that are critical to global stability.

In the alternate path method, structural integrity is assessed through analysis, to ascertain whether the structural system can bridge over failed structural members. For example, if a column is damaged,

continuity of the beams adjacent to the top of the damaged column is required to redistribute the loads previously carried by the damaged column. The analysis must demonstrate the adequacy of the beams and their connections to redistribute these loads, potentially through catenary action. An accurate characterization of the nonlinear, large-deformation behavior associated with the transfer of forces through the connections in such scenarios is critical in assessing the potential for disproportionate collapse. Physical tests are indispensable in validating the analytical models used to represent nonlinear connection behavior in such scenarios.

This section describes some of the recent NIST research in the area of mitigation of disproportionate collapse including both full-scale testing and finite element-based modeling of steel and reinforced concrete beam-column assemblies. Each assembly comprises three columns and two beams, representing a portion of the second floor framing of a prototype ten-story building. Both assemblies represent portions of intermediate moment frames (IMFs) designed for Seismic Design Category C (SDC C), typical of the Atlanta, Georgia area. The beam-column assemblies are subjected to monotonically increasing vertical displacement of the unsupported center column to observe their behavior under a simulated column removal scenario, including the development of catenary action in the beams. Each test is continued until a collapse mechanism of the assembly is reached. Both detailed and reduced finite element models of the test specimens are developed, and the model predictions show good agreement with the experimental results, providing validation of the modeling approaches. The reduced models are used to analyze complete structural systems under column removal scenarios, and results are presented from dynamic analysis of sudden column removal. Such modeling capabilities are valuable for assessing the vulnerability of structural systems to disproportionate collapse, and evaluating the risk of collapse for structures exposed to abnormal loads.

Description of Building Designs

A rectangular plan of 30.5 m by 45.7 m was chosen for all prototype buildings. The steel prototype building was designed and detailed in accordance with the American Institute of Steel Construction Seismic Provisions (AISC 2002). The building used IMFs at the perimeter for the lateral-load resisting system and gravity frames on the interior. Welded unreinforced flange-bolted web (WUF-B) connections were used in the moment frames, selected from prequalified steel connections specified in FEMA 350 (FEMA 2000a). ASTM A992 structural steel, with a minimum specified yield strength of $F_y = 345$ MPa, was used in all beams and columns. ASTM A36 steel ($F_y = 248$ MPa) was used for the shear tabs and continuity plates at the beam-to-column joints. ASTM A490 high strength bolts were used for the bolted connections, and welding requirements followed the recommendations in FEMA 353 (FEMA 2000b).

The concrete prototype building was designed and detailed in accordance with the American Concrete Institute's Building Code Requirements for Structural Concrete (ACI 2002). The building used IMFs for the lateral-load resisting system. The building was designed using normal weight concrete having a specified compressive strength of 27.6 MPa and ASTM A615 reinforcing steel ($F_y = 414$ MPa).

Steel Beam-Column Assembly

The steel test assembly comprised two W21x73 beams connected to three W18x119 columns by WUF-B connections. The span length (center to center of columns) of the beams was 6.10 m. The WUF-B connection is similar to the connection commonly used prior to the 1994 Northridge earthquake. FEMA 355D (FEMA 2000c) provides extensive information on testing and performance of WUF-B connections under cyclic loading. Details of the WUF-B connection used in the test are shown in Figure 1. The beam web is connected to the column flange using a shear plate (shear tab), which is welded to the column using an 8 mm fillet weld and bolted to the beam web using three 25 mm diameter ASTM A490 bolts. The bolt holes are standard holes with an edge distance of

70 mm. The beam flanges are joined to the column flange using complete joint penetration (CJP) groove welds. Weld access holes are cut from the beam webs according to the recommendations of FEMA 350 (FEMA 2000a). Continuity plates are provided for both interior and exterior columns as shown in Figure 1. No doubler plates were required. A schematic of the test setup for the steel beam-column assembly is shown in Figure 2. Figure 3 shows photographs of the steel assembly, including a close-up view of the connections to the center column.

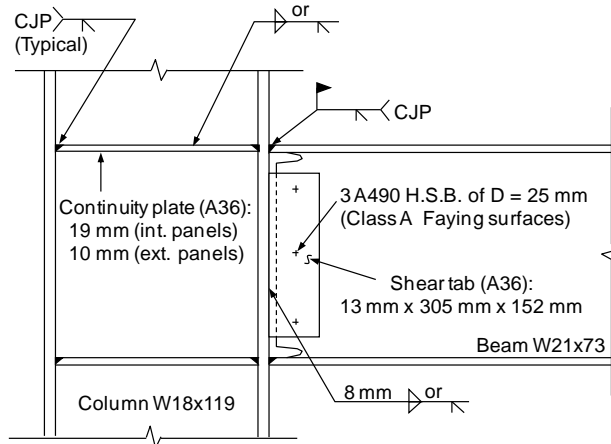


Figure 1: WUF-B connection details for the steel assembly.

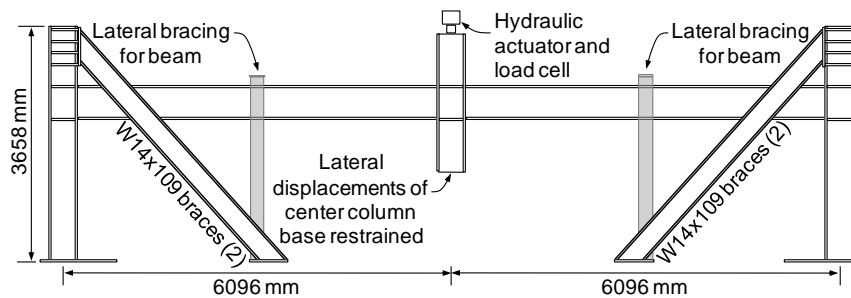


Figure 2: Test setup for the steel assembly.



Figure 3: Photographs of the steel assembly test.

The bases of the exterior columns were anchored to the strong floor of the test facility, and the tops were rigidly attached to two diagonal braces to restrain horizontal movement. The base of the center stub column was unrestrained vertically, but out-of-plane movement was restrained. In addition, the beams were restrained from out-of-plane movement at mid-span by lateral bracing. A hydraulic actuator with a capacity of 2670 kN and stroke of 508 mm was attached to the top of the center column to apply a vertical load to the assembly. Load was applied under displacement control at a rate of 25 mm/min. The estimated uncertainty in the measured data from the load cells, deflection gages,

strain gages, and inclinometers was $\pm 1\%$. More details on the testing setup and instrumentation are provided in Lew et al. (2013).

Test results

Under prescribed vertical displacement of the center column, the assembly experienced large deflections and rotations prior to failure. The connection failed at a vertical displacement of the center column of about 495 mm. At that displacement, the applied vertical load was about 890 kN. The connection failed in the following sequence (see Figure 4): (1) local buckling of the top flanges of the beams at the center column, (2) successive shear fractures of the lowermost and middle bolts connecting the beam web to the shear tab, and (3) fracture of the bottom flange near the weld access hole.

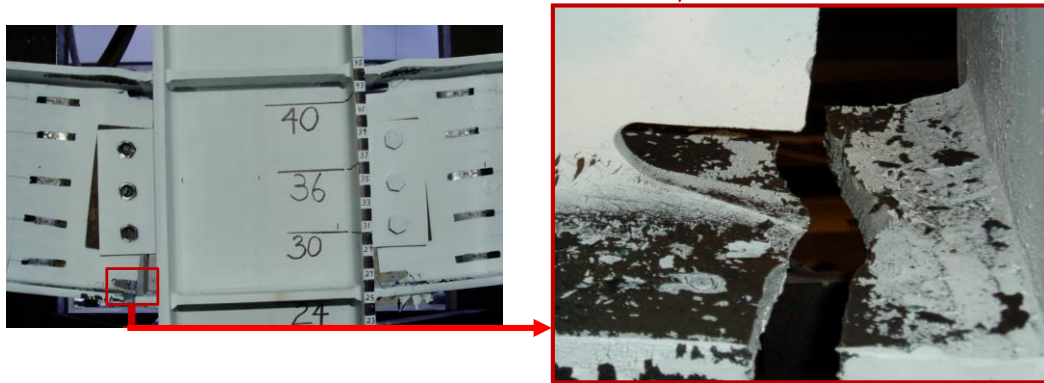


Figure 4: Failure mode of the steel assembly.

Plots of the applied vertical load versus vertical displacement of the center column and the beam axial force versus the vertical displacement of the center column are shown in Figure 5. Experimental measurements are presented along with finite element model predictions that are discussed subsequently. The experimental beam axial force is calculated based on measured strains in the beams. As the plots indicate, the assembly was unloaded at a vertical displacement of about 460 mm, to adjust the stroke of the hydraulic ram, and was then reloaded to failure. Figure 5 indicates that the assembly remained in the elastic range up to a vertical displacement of the center column of about 50 mm. In the early stages of loading, the behavior of the assembly was primarily flexural. As the loading progressed with increased vertical displacement of the center column, the response of the assembly was dominated by catenary action, as indicated by the development of axial tension in the beams. At the time of failure, the axial tension in the beams was about 667 kN.

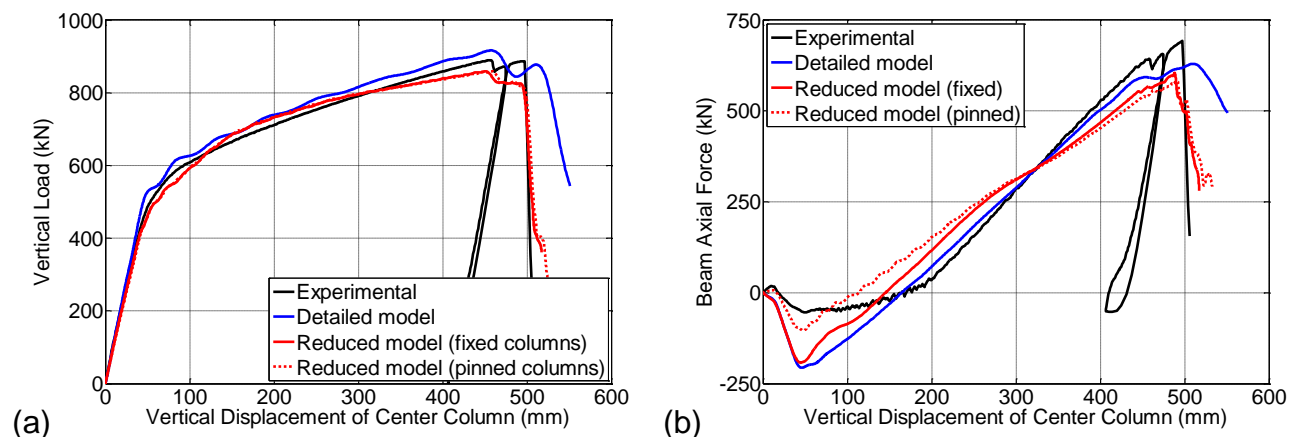


Figure 5: (a) Vertical load and (b) beam axial force versus vertical displacement of center column for the steel assembly.

Finite element models

Two finite element models of the beam-column assembly with WUF-B connections were developed to study the behavior of the connections and to compare the calculated response with experimental values. The first was a detailed model of the assembly with approximately 300 000 elements, while the second was a reduced model with about 150 elements. The analyses were conducted using LS-DYNA¹, an explicit formulation, finite element software package (Hallquist 2007). Overviews of both models are shown in Figure 6.

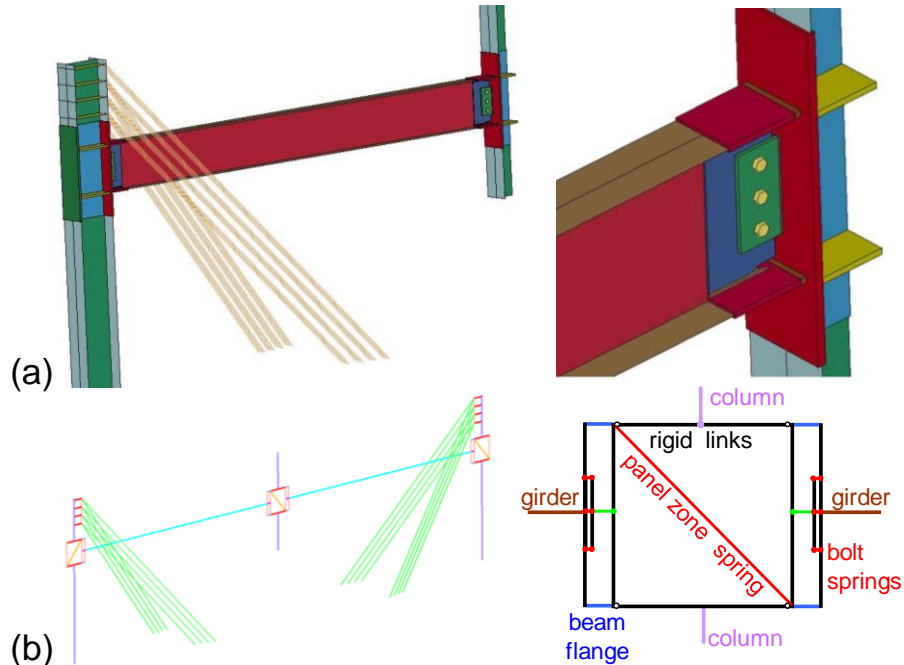


Figure 6: (a) Detailed and (b) reduced models of the steel assembly.

The detailed model, shown in Figure 6(a), consisted of finely meshed solid elements representing the beams, columns, continuity plates, shear tabs, bolts, and welds in the vicinity of the connection. Contact with friction was defined between the bolts, shear tabs, and beam webs to model the transfer of forces through the bolted connection. Away from the connection zones, the beams and columns were modeled with shell elements. Spring elements were used to model the braces at the top of the exterior columns. All nodes were fixed at the bases of the exterior columns. In order to reduce the time required for computation, only half of the assembly was modeled, with appropriate boundary conditions enforced along the plane of symmetry. The steel for the various elements was modeled using a piecewise-linear plasticity model based on coupon test data obtained for all steel sections and plates. Fracture was modeled using element erosion.

The reduced model used Hughes-Liu beam elements (Hallquist 2007) to model the beams and columns, as well as the shear tabs and beam flanges in the connection regions. The steel was modeled using a piecewise-linear plasticity model based on coupon test data, and fracture was modeled using element erosion. An arrangement of beam and spring elements, connected with rigid links, was used to

¹ Certain commercial entities, equipment, or materials may be identified in this document in order to describe an experimental procedure or concept adequately. Such identification is not intended to imply recommendation or endorsement by the National Institute of Standards and Technology, nor is it intended to imply that the entities, materials, or equipment are necessarily the best available for the purpose.

model the WUF-B connection as shown in Figure 6(b). Nonlinear spring elements were used to model the shear behavior of the bolts, along with bearing-induced deformations of the shear tab and beam web. The shear load-deformation curve for these spring elements was based on the results of a detailed solid-element model of the bolted connection (Sadek et al. 2010). Spring elements were also used to model the diagonal braces and the shear behavior of the panel zone. For the panel zone, the diagonal springs had an elasto-plastic load deformation curve based on the geometry and strength of the panel zone. Further details are provided in Sadek et al. (2010, 2013). Two analyses were conducted in which the bases of the exterior columns were modeled as either fixed or pinned.

Based on the analysis of the detailed model, the beam-column assembly responded initially in a purely flexural mode before catenary action developed. The beam remained essentially elastic except for the sections in the vicinity of the connections to the center and exterior columns, where significant yielding was observed. The failure mode of the connection based on this analysis, shown in Figure 7, was very similar to that observed in the experiment (Figure 4). The results from the reduced model were consistent with those from the detailed model, albeit without the same level of detail. In Figure 5 comparisons are presented between the finite element model predictions and the experimental measurements of the vertical load and the beam axial force, plotted against the vertical displacement of the center column. The plots indicate a good agreement between the experimental and computational results and provide validation for the detailed and reduced models.

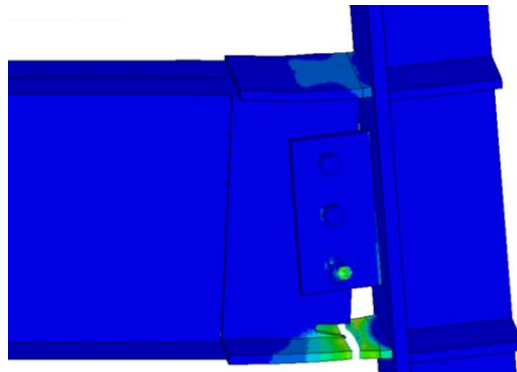


Figure 7: Failure mode from detailed model of the steel assembly.

Reinforced Concrete Beam-Column Assembly

The reinforced concrete test assembly for the IMF frames comprised two 711 mm by 508 mm beams supported by three 711 mm by 711 mm columns as shown in Figure 8. The span length of the beams (center-to-center of columns) was 6.10 m. A schematic of the test setup used for the concrete beam-column assembly is shown in Figure 9. Figure 10 shows a photograph of the reinforced concrete assembly in the initial position.

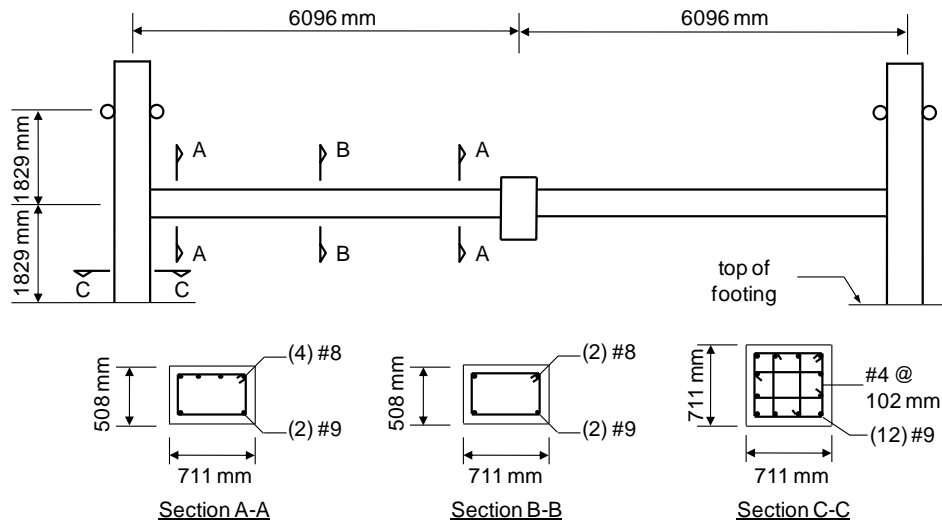


Figure 8: Schematic of the reinforced concrete assembly.

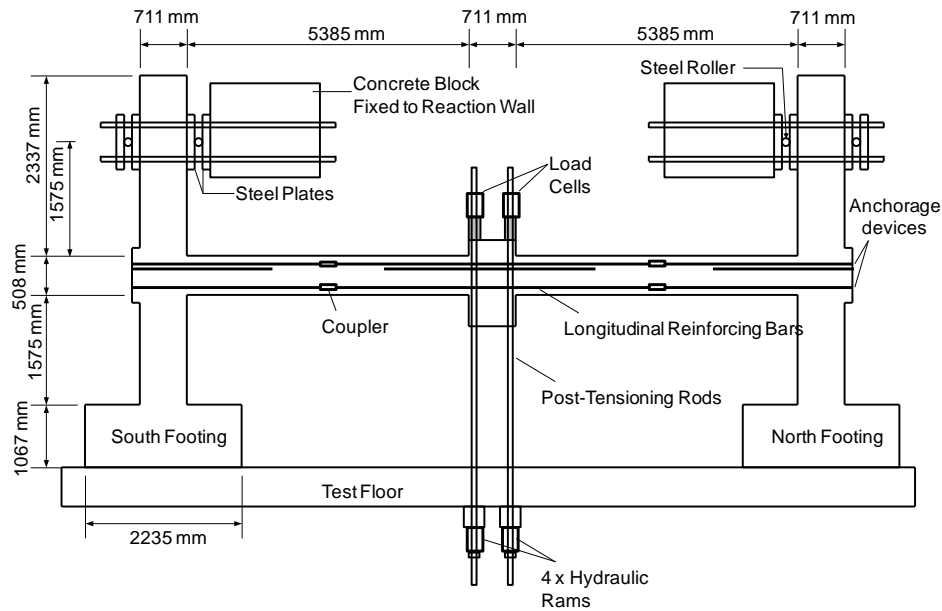


Figure 9: Test setup for the reinforced concrete assembly.



Figure 10: Photograph of the reinforced concrete assembly in the initial position.

As shown in Figure 9, the load was applied to the center stub column by means of four post-tensioning rods that were pulled down by four hydraulic rams, each having a capacity of 534 kN and a stroke of 102 mm. Because this loading scheme is self-centering, lateral bracing of the center stub column was not required. The load was applied under displacement control at a rate of 25 mm/min. The estimated

uncertainty in the measured data from the load cells was $\pm 1\%$. The tops of the exterior columns were restrained from horizontal movement by steel rollers (see Figure 9), while vertical motion was permitted. The bases of the exterior columns were fixed to large footings which in turn were anchored to the test floor. Both top and bottom longitudinal beam reinforcing bars were spliced with threaded couplers at mid-span of the beams. Mechanical bar couplers were used instead of lap splices in order to evaluate their effectiveness in the development of catenary action. All longitudinal beam reinforcing bars were anchored at the exterior beam-column joints by means of threaded mechanical anchorage devices. These anchorage devices are supplemented with 19 mm thick steel plates as shown in Figure 9. Further details on the testing setup and instrumentation are provided by Lew et al. (2011, 2013).

Test results

Figure 11(a) shows a plot of the vertical load versus the vertical displacement of the center column. Experimental measurements are presented along with model predictions that will be discussed subsequently. As the load was increased, flexural cracks developed in the tension zones, at the top of the beams adjacent to the exterior columns and at the bottom of the beams adjacent to the center column. Yielding of the longitudinal reinforcing bars in the cracked regions was first detected at about 267 kN. The load reached an initial peak of 296 kN at a vertical displacement of 127 mm and started to decrease with additional displacement. This decrease in load was associated with crushing of concrete at the top of the beams adjacent to the center column. The load leveled at 196 kN at a displacement of 406 mm. With further increases in displacement, the load began to increase again due to the development of catenary action, while the cracks at the bottom of the beams near the center column widened. The assembly attained a maximum load of 547 kN at a vertical displacement of 1090 mm, at which point the assembly failed due to rupture of one of the bottom bars. A second bar ruptured at a displacement of 1130 mm (see Figure 12).

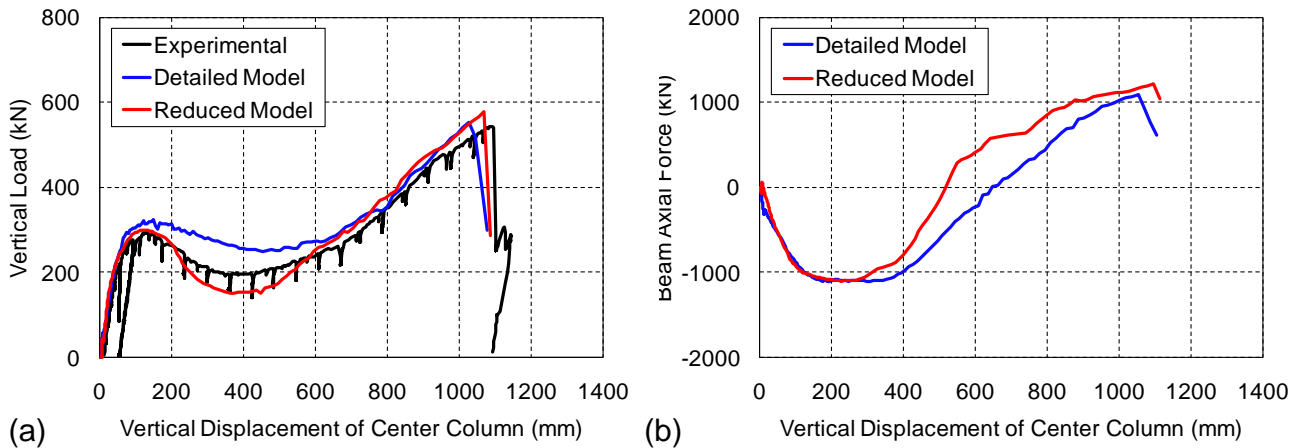


Figure 11: Vertical load and beam axial force versus vertical displacement of center column for the reinforced concrete assembly.



Figure 12: Failure mode of the reinforced concrete assembly.

Finite element models

The reinforced concrete assembly was modeled using two different approaches: a detailed finite element model with approximately 70 000 elements and a reduced component-based model with about 150 elements. Calculated structural responses were compared to those measured from the experiment. The analyses were conducted using LS-DYNA (Hallquist 2007). Overviews of both models are shown in Figure 13.

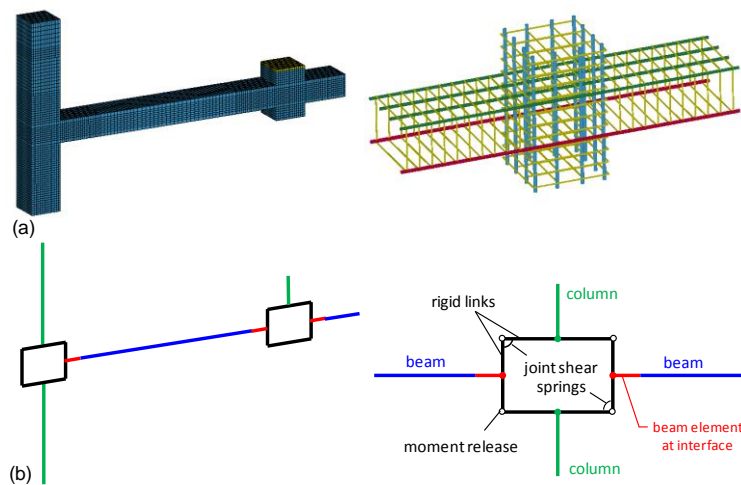


Figure 13: (a) Detailed and (b) reduced models of the reinforced concrete assembly.

In the detailed model, concrete was represented by finely meshed solid elements and reinforcing bars were modeled as beam elements. A contact interface between beam elements and solid elements was defined to describe the bond-slip behavior of reinforcing bars in the beams. The bottom of the exterior columns was assumed fixed. Since the tops of the exterior columns were restrained horizontally by steel rollers (see Figure 9), contact was defined between the columns and rigid cylinders representing the rollers. Steel properties of reinforcing bars were modeled using a piecewise-linear plasticity model based on test data, and fracture was modeling using element erosion. The concrete material was modeled by a continuous surface cap model (material 159 in LS-DYNA).

In the reduced model, the beams and columns were modeled using beam elements with fiber-discretized sections. An arrangement of beams, spring elements, and rigid links was used to simulate the behavior of beam-column joints. Joint shear was represented by rotational springs. Critical sections

at the beam-to-column interface were modeled using a beam element with bond-slip effect incorporated into the material property of the reinforcing bars (Bao et al. 2013).

The failure mode predicted by both the detailed and reduced models was fracture of the longitudinal bottom bars of the beams near the center column, as shown in Figure 14 for the detailed model. These predictions were consistent with the failure mode observed in the test (see Figure 12). In Figure 11(a) comparisons are presented between the model predictions and the experimental measurements of the applied vertical load, plotted against the vertical displacement of the center column. The agreement between the experimental and computational results is good and provides validation for the detailed and reduced models. The plots show that the models are able to correctly predict significant softening after an initial peak load, with subsequent increases in load due to catenary action. Catenary action is indicated by the increasing axial tension evident in Figure 11(b), which shows model predictions of the beam axial force versus the vertical displacement of the center column. In the early stages of loading, the beam is predominantly in compression due to arching action, and subsequently the compression force is reduced due to softening and crushing of concrete. As the loading progresses with increased vertical displacement of the center column, the response of the assembly is dominated by catenary action. The different stages of response are further discussed by Bao et al. (2013).

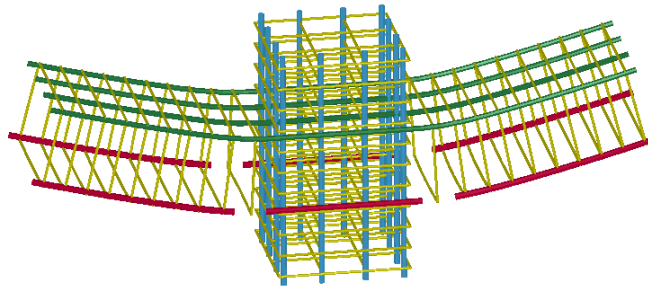


Figure 14: Failure mode from detailed model of the reinforced concrete assembly.

System Analyses

Because the reduced models described above can be analyzed much more rapidly than the detailed models, they are used here in the analysis of complete structural systems. To assess the robustness of structural systems, a dynamic column removal, involving sudden removal of selected columns under service loads was conducted. Figure 15 shows peak vertical displacements after dynamic removal of two first-story columns for a 10-story steel IMF building. The removed columns were part of a perimeter IMF. The structural system was able to withstand this column loss without collapse, limiting the peak vertical displacement to about 360 mm.

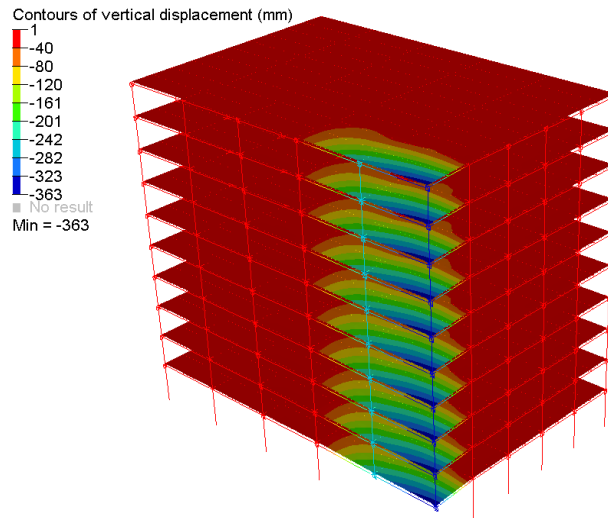


Figure 15: Peak vertical displacements of steel IMF building after dynamic removal of two columns.

Discussion

This section presented both full-scale testing and finite-element based modeling of steel and reinforced concrete beam-column assemblies. The steel assembly, which incorporated welded, unreinforced flange, bolted web connections, exhibited a fairly well-defined yield point at a vertical displacement of about 50 mm, and a gradually increasing load beyond the yield point up to failure at an ultimate load of 890 kN. The observed hardening behavior beyond the yield point was associated with the development of catenary action, and a peak axial tension value of about 670 kN was measured in the beams of the steel assembly. The reinforced concrete assembly failed at a vertical column displacement of 1090 mm, with a corresponding ultimate load of 547 kN. The vertical load versus displacement curve of the reinforced concrete assembly exhibited softening behavior, with an initial peak load at a vertical displacement of about 100 mm and reductions in load thereafter, up to a displacement of about 500 mm, at which point the load began to increase again up to the point of failure. The observed softening behavior was associated with softening and crushing of concrete, while the subsequent hardening behavior was associated with the development of catenary action.

Both detailed and reduced finite element models of the assemblies were developed, and the computational predictions showed good agreement with the experimentally observed response characteristics and failure modes, providing validation of the modeling approaches. The detailed models involved hundreds of thousands of solid and/or shell elements and were capable of representing the behavior and failure of the assemblies in great detail. The reduced models, which involved on the order of a hundred beam and spring elements, also accurately captured the behavior and failure modes of the assemblies, while analyses with the reduced models can be executed much more rapidly. The validated reduced models developed in this study are being used in the analysis of complete structural systems to assess their reserve capacity and robustness.

FIRE PERFORMANCE OF STRUCTURES

Losses due to fire cost the U.S. economy approximately \$328B in 2010 (Hall 2013). Yet, current building design practice does not consider fire as a design condition for structures. Rather, required fire ratings of building components and assemblies derived from standard fire endurance tests, such as ASTM E-119, are specified in current building codes. Currently, there are no science-based, accepted measurement tools to evaluate the fire performance of entire structures, including connections, under realistic fire scenarios. The state of the art in measurement science to predict structural performance to failure under extreme loading conditions such as in an uncontrolled fire is lacking. This can lead to

significant safety concerns. Thus, there is an urgent and critical need to develop and implement improved standards, methodologies, and tools that explicitly consider realistic building fire loads, both in the design of new structures and in the rehabilitation of existing structures. As a result of its recent investigation of the collapse of the WTC towers and WTC 7, NIST has recommended the development of performance-based standards and code provisions, as an alternative to current prescriptive design methods, to enable the design and rehabilitation of structures to resist real building fire conditions, and the development of tools, guidelines, and test methods necessary to evaluate the fire performance of the structure as a whole system. A key recommendation resulting from the investigation of WTC 7 was that careful consideration should be given to the possibility that certain design features (e.g., long span floor systems, connections that cannot accommodate thermal effects, etc.) may adversely affect the performance of the structural system under fire conditions.

Analysis of structural systems under fire conditions involves the prediction of performance of the entire structural system at, or near, its limit state of collapse as an uncontrolled fire is considered an extreme (rare though not improbable) event. Development of accurate models to predict complex structural system behavior resulting from the effects of thermal expansion and diminished mechanical properties at elevated temperatures requires the availability of robust computational models, validated against large-scale tests under real fire exposures. At the present time, experimental data on the behavior of connections, members, and systems under realistic building fire conditions are lacking. In addition, detailed modeling of a complete structural system to failure imposes large computational demands. Reduced models of key structural components such as connections that capture the predominant behaviors and failure modes at elevated temperatures are needed for cost effective assessment of structural response to fire and resistance to collapse in an uncontrolled fire. Development and validation of such models pose a challenge.

Computational Tools

As part of its investigation into the collapse of the World Trade Center (WTC) buildings, NIST conducted a comprehensive modeling of the fire effects on the two towers WTC 1 and WTC 2, as well as WTC 7. A specific objective of the WTC investigation was to determine why the WTC buildings collapsed. A series of detailed analyses was performed, consisting of: (1) a fire dynamics simulation to model the spread and growth of the fires with time (Figure 16), (2) a thermal analysis to predict the temporal and spatial distribution of temperature (temperature time-histories at every node) in the structure (Figure 17), and (3) a structural analysis consisting of a finite element analysis to simulate the response of the structure to the fire-induced temperature histories that led to collapse initiation (Figure 18).

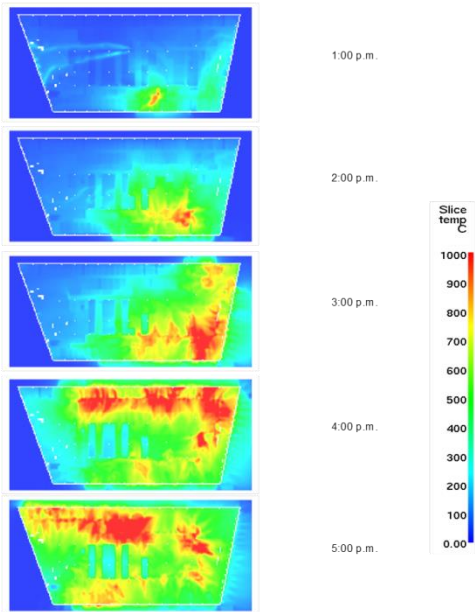


Figure 16: Progression of simulated fire in WTC 7 with upper layer gas temperatures shown.

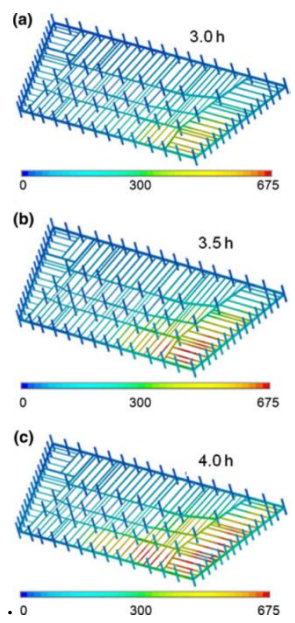


Figure 17: Temperatures (°C) of floor framing between 3.0 h and 4.0 h of heating in the thermal analysis.

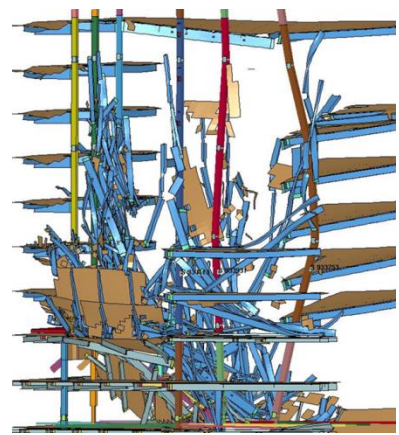


Figure 18: Buckling of interior columns on the east side of WTC 7 that initiated the collapse sequence.

The structural models were developed in ANSYS (2007) to determine the pseudo-static structural response to spatially and temporally varying fire-induced gas temperatures, and to predict the resulting local structural failures. The pseudo-static model accounted for temperature-dependent material property degradation and component failure mechanisms. Failure criteria were developed to identify when a structural component was no longer contributing to the strength or stiffness of the structural system and was removed to prevent extreme impedance of analysis convergence.

The structural models had the following features:

- Representations of columns, beams, girders, composite floor slab, and connections.
- Geometric and material nonlinearities, including temperature-dependent material properties, and thermal expansion and contraction.
- Evolving temperature states, which included heating and cooling phases, input as a temperature time history for each node, distinct from other nodes, at 5 min intervals for WTC 1 and WTC 2 and at 30 min intervals for WTC 7 with linear interpolation between temperature states.
- Connection models that simulated failure of connection components.
- Failure criteria for connections, shear studs within a composite floor system, buckling instability of beams and girders, and concrete cracking and crushing in floor slabs.

Beams, girders, and columns were modeled with a 3-D linear finite strain beam element that is well suited for large rotation and/or large strain nonlinear solutions. Floor slabs were modeled with a 4-node finite strain shell element. Temperature-dependent inelastic material properties were used for beam and shell elements. Connection and shear stud models included in the models using a combination of rigid beams, contact elements, control elements, spring elements, and user-defined “break elements”, which modeled component failure. A control element is unidirectional and can turn on/off during an analysis to connect or disconnect parts of the connection model. A break element has a multi-degree of freedom elastic spring with the capability of disconnecting once its capacity is reached. Break elements were developed to simulate complex modes of failure in connections using relatively few degrees of freedom.

The temperature-dependent force and moment capacity of a break element was defined with a temperature-dependent reduction factor. Different tensile and compressive capacities were assigned to connections where appropriate. Connections with multiple failure modes required several break elements connected in series and/or parallel as determined by the logical sequence of partial failures prior to the total failure of the connection (Figure 19). The inclusion of contact elements in the connection models allowed for slip and construction clearances (gaps) to be taken into account and thus insured different responses to tensile and compressive loads.

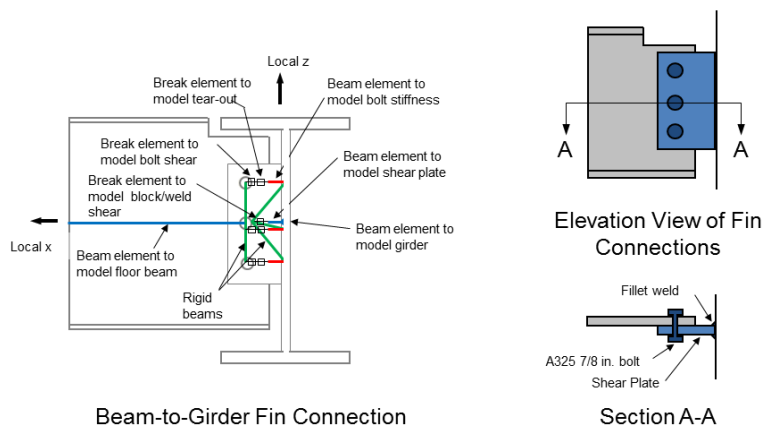


Figure 19: Analytical model for a fin connection in WTC 7.

The structural models were used to conduct a series of analyses on the WTC buildings to understand the response characteristics of the structural systems and to develop hypotheses for the collapse of the buildings. More details can be found in NIST (2005) and NIST (2008).

Experimental Facilities

The National Fire Research Laboratory (NFRL), located on the National Institute of Standards and Technology (NIST) Gaithersburg campus, is a unique-in-the-world facility for conducting critical, problem-focused, real-scale experimental research to provide the technical basis for improvements in building fire standards, codes, and practices associated with the interaction of structural systems with fire.

A study was commissioned by NIST in 2002 to identify existing facilities in the U.S. and elsewhere that were properly equipped to test the structural performance of real-scale assemblies and systems commonly used in building construction (Beitel and Iwankiw, 2008) under actual fire conditions. None were located with the capability to conduct well controlled experiments on three-dimensional real-scale structural systems exposed to realistic fire conditions. The need for such a facility was highlighted by the Society of Fire Protection Engineers (NISTIR 7133) and was specifically included as a recommendation in the final report on the September 11, 2001 collapse of the World Trade Center towers (NIST, 2005).

Large fire research studies have been conducted in the NFRL for more than 30 years without the capability to apply controlled mechanical loads on test structures. The facility is now being expanded with the addition of 1965 m² of new laboratory space to include this capability and meet the needs identified in the SFPE roadmap and the recommendation from the WTC study. The expanded NFRL (Figure 20) is currently under construction and is scheduled for completion in 2013, followed by a 12 month commissioning phase. When fully operational, the NFRL will provide new and unique experimental capabilities for real-scale structural systems up to 9 m high constructed on a strong floor that is 18 m by 27 m in plan. The laboratory is designed to provide multi-axial mechanical loading using hydraulic actuators with a maximum capacity of 1.5 MN and thermal loads of up to 20 MW continuously for four hours. A CAD rendering of the test area showing the strong floor, strong wall and 20 MW calorimeter hood is shown in Figure 21. The experimental facility will maintain tight control on and precision measurement of the thermal and mechanical loads, and of the response of the structure to these loads as a function of time.

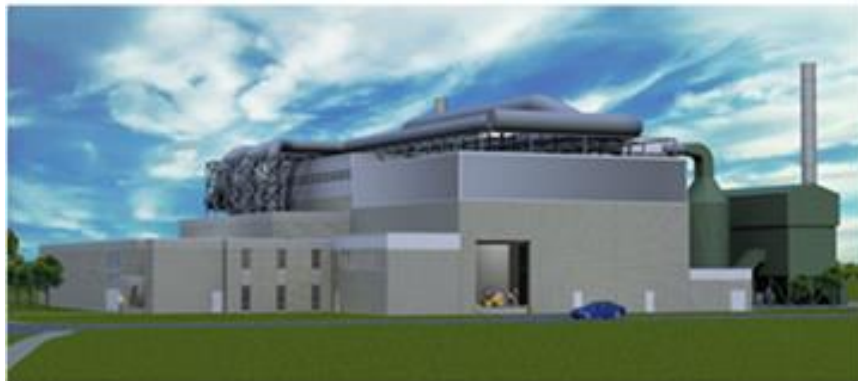


Figure 20: Exterior view of expanded National Fire Research Laboratory.

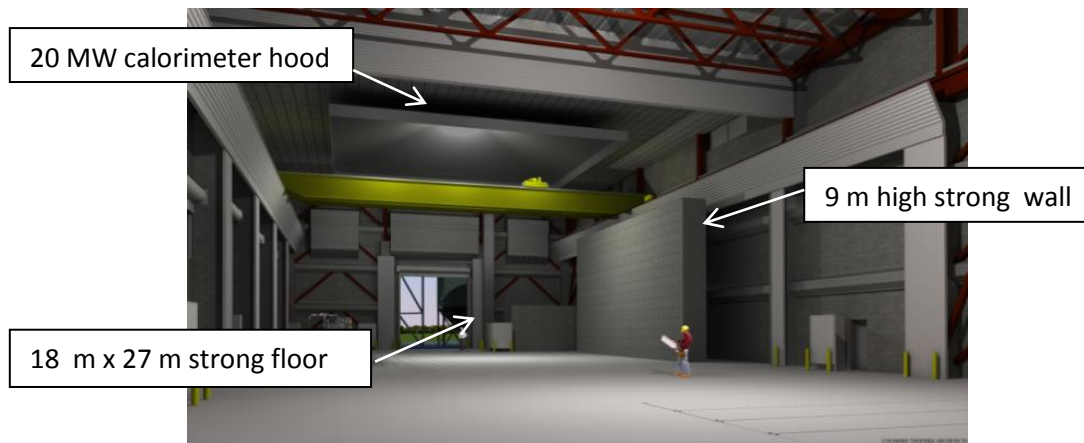


Figure 21: Interior view of expanded National Fire Research Laboratory.

The scientific objectives of the NFRL are to develop an experimental database on the performance of materials, components, connections, assemblies and systems under fire loading and to gain knowledge, quantify performance, and validate physics-based predictive models, including a library of component and connection models for use in performance-based design. Data from experiments conducted in the NFRL will provide the technical basis for performance metrics; acceptance criteria for different levels of performance objectives; mitigation strategies based on evaluated performance to provide adequate fire protection for the structure; and the measurement science to support a transformation from prescriptive to performance-based standards in design of structures for fire resistance.

The NFRL is designed for conducting experiments on steel, concrete and composite structural assemblies and systems. It can also be used for experiments on timber construction and on polymeric-based composite structures, on load-bearing wall assemblies, and for experiments on materials for enhancing fire resistance (e.g., SFRM, gypsum board, and intumescent). Designs and materials for buildings, bridges, and tunnel sections are all within scope.

SUMMARY

This paper presented a brief overview of research at the National Institute of Standards and Technology (NIST) on disaster resilience of buildings, infrastructure, and communities, including component programs and projects. NIST's efforts aim at developing the scientific basis required to enable technological innovation, improve predictive capabilities, and improve codes, standards, and practices for the cost-effective improvement of disaster resilience, including life-safety and reduction of property loss due to natural and man-made hazards. The fundamental idea underpinning this research is that disaster resilience can be enhanced by developing a robust capability to predict the effects of hazards on the performance of complex structural systems. This will be achieved by providing data to characterize the hazard, validated models to predict performance, metrics for measuring performance, acceptance criteria for differing levels of performance objectives, and mitigation strategies based on performance evaluation. Special emphasis was provided for two key research efforts related to structural design for disaster resilience currently underway at the NIST. These included mitigation of disproportionate collapse and fire performance of structures. For each effort, an overview was provided, followed by details of recent work carried out by the NIST including experiments and computational studies for the assessment of disproportionate collapse potential and the design and construction of the National Fire Research Laboratory (NFRL).

REFERENCES

- ASCE (2010). *Minimum Design Loads for Buildings and Other Structures*, SEI/ASCE 7-10, American Society of Civil Engineers, Reston, VA.
- ACI (2002). *Building Code Requirements for Structural Concrete (ACI 318-02)*, American Concrete Institute, Farmington Hills, MI.
- AISC (2002). *Seismic Provisions for Structural Steel Buildings*, American Institute of Steel Construction, Chicago, IL.
- ANSYS (2007). ANSYS Mechanical Release 11.0, ANSYS Inc., Southpointe, 275 Technology Drive, Canonsburg, PA
- Bao, Y., Lew, H.S., and Kunnath, S.K. (2013). "Modeling of reinforced concrete assemblies under a column removal scenario." *Journal of Structural Engineering*, in press.
- Beitel, J. and Iwankiw, N. (2008). *Analysis of Needs and Existing Capabilities for Full-scale Fire Resistance Testing*, NIST GCR 02-843-1.
- DOD (2009). *Design of Buildings to Resist Progressive Collapse, Unified Facilities Criteria (UFC) 4-023-03*, Department of Defense, 25 January 2009.
- FEMA (1996). *The Oklahoma City Bombing: Improving building performance through multi-hazard mitigation*, FEMA Report 277, Federal Emergency Management Agency, Washington, D.C.
- FEMA (2000a). *Recommended Seismic Design Criteria for New Steel Moment-Frame Buildings*, FEMA 350, SAC Joint Venture and Federal Emergency Management Agency, Washington, D.C.
- FEMA (2000b). *Recommended Specifications and Quality Assurance Guidelines for Steel Moment-Frame Construction for Seismic Applications*, FEMA 353, SAC Joint Venture and Federal Emergency Management Agency, Washington, D.C.
- FEMA (2000c). *State of the Art Report on Connection Performance*, FEMA 355D, SAC Joint Venture and Federal Emergency Management Agency, Washington, D.C.
- GSA (2003). *Progressive Collapse Analysis Design Guidelines for New Federal Office Buildings and Major Modernization Projects*, General Services Administration, Washington, D.C.
- Hall, J. (2013). *The total cost of fire in the United States*, National Fire Protection Association, Quincy, MA.
- Hallquist, J. (2007). *LS-DYNA Keyword User's Manual*, Livermore Software Technology Corporation, Livermore, CA, Version 971.
- Lew, H.S., Bao, Y., Sadek, F., Main, J.A., Pujol, S., and Sozen, M.A. (2011). "An experimental and computational study of reinforced concrete assemblies under a column removal scenario." *NIST Technical Note 1720*, National Institute of Standards and Technology, Gaithersburg, MD.
- Lew, H.S., Bao, Y., Pujol, S., and Sozen, M.A. (2013). "Experimental study of RC assemblies under a column removal scenario." *ACI Structural Journal*, in press.
- Lew, H.S., Main, J.A., Robert, S.D., Sadek, F., Chiarito, V.P. (2013). "Performance of steel moment connections under a column removal scenario. I: Experiments." *Journal of Structural Engineering*, 139(1), 98-107.
- NIST (2005). *Final Report of the Collapse of the World Trade Center Towers*, NIST NCSTAR 1, National Institute of Standards and Technology, Gaithersburg, MD.
- NIST (2008). *Final Report of the Collapse of World Trade Center Building 7*, NIST NCSTAR 1A, National Institute of Standards and Technology, Gaithersburg, MD.
- NISTIR 7133 (2004). *NIST-SFPE Workshop for Development of a National R&D Roadmap for Structural Fire Safety Design and Retrofit of Structures: Proceedings*, Gaithersburg, MD.
- Sadek, F., Main, J.A., Lew, H.S., Robert, S.D., Chiarito, V.P., El-Tawil, S. (2010). "An experimental and computational study of steel moment connections under a column removal scenario." *NIST Technical Note 1669*, National Institute of Standards and Technology, Gaithersburg, MD.
- Sadek, F., Main, J.A., Lew, H.S., El-Tawil, S. (2013). "Performance of steel moment connections under a column removal scenario. II: Analysis." *Journal of Structural Engineering*, 139(1), 108-119.